Roles of nicotinic acetylcholine receptor β subunits in function of human α4-containing nicotinic receptors

Jie Wu[1], Qiang Liu[1], Kewei Yu[1], Jun Hu[1], Yen-Ping Kuo[2], Marsha Segerberg[3], Paul A. St John[4] and Ronald J. Lukas[2]

[1]*Division of Neurology and* [2]*Division of Neurobiology, Barrow Neurological Institute, St. Joseph's Hospital and Medical Center, Phoenix, AZ 85013-4496, USA*

[3]*Division of Science, Chandler-Gilbert Community College, Chandler, AZ 85225, USA*

[4]*Department of Cell Biology and Anatomy, University of Arizona, Tucson, AZ 85724-5017, USA*

Naturally expressed nicotinic acetylcholine receptors (nAChR) containing α4 subunits (α4*-nAChR) in combination with β2 subunits (α4β2-nAChR) are among the most abundant, high-affinity nicotine binding sites in the mammalian brain. β4 subunits are also richly expressed and colocalize with α4 subunits in several brain regions implicated in behavioural responses to nicotine and nicotine dependence. Thus, α4β4-nAChR also may exist and play important functional roles. In this study, properties were determined of human α4β2- and α4β4-nAChR heterologously expressed *de novo* in human SH-EP1 epithelial cells. Whole-cell currents mediated via human α4β4-nAChR have ∼4-fold higher amplitude than those mediated via human α4β2-nAChR and exhibit much slower acute desensitization and functional rundown. Nicotinic agonists induce peak whole-cell current responses typically with higher functional potency at α4β4-nAChR than at α4β2-nAChR. Cytisine and lobeline serve as full agonists at α4β4-nAChR but are only partial agonists at α4β2-nAChR. However, nicotinic antagonists, except hexamethonium, have comparable affinities for functional α4β2- and α4β4-nAChR. Whole-cell current responses show stronger inward rectification for α4β2-nAChR than for α4β4-nAChR at a positive holding potential. Collectively, these findings demonstrate that human nAChR β2 or β4 subunits can combine with α4 subunits to generate two forms of α4*-nAChR with distinctive physiological and pharmacological features. Diversity in α4*-nAChR is of potential relevance to nervous system function, disease, and nicotine dependence.

(Resubmitted 2 June 2006; accepted 5 July 2006; first published online 6 July 2006)

Corresponding author J. Wu: Neurophysiology Laboratory, Division of Neurology, Barrow Neurological Institute, 350 West Thomas Road, Phoenix, AZ 85013-4496, USA. Email: jie.wu@chw.edu

Nicotinic acetylcholine receptors (nAChR) in mammals exist as a diverse family of molecules composed of different combinations of subunits derived from at least 16 genes (see reviews by Lukas *et al.* 1999; Jensen *et al.* 2005). nAChR are prototypical members of the ligand-gated ion channel superfamily of neurotransmitter receptors and models used to establish concepts pertaining to mechanisms of drug action, synaptic transmission, and structure and function of transmembrane signalling molecules. The most abundant form of heteromeric nAChR in the brain contains α4 and β2 subunits (α4β2-nAChR; Whiting & Lindstrom, 1987; Flores *et al.* 1992; Gopalakrishnan *et al.* 1996; Lindstrom, 1996) although additional subunits may integrate into these complexes. α4β2-nAChR bind nicotine with high affinity, and respond to levels of nicotine found in the plasma of smokers (Benowitz *et al.* 1989; Hsu *et al.* 1995; Lindstrom, 1996; Fenster *et al.* 1997; Lukas *et al.* 1999; Jensen *et al.* 2005; Lukas, 2006). They have been implicated in nicotine self-administration, reward, and dependence, and in diseases such as Alzheimer's disease and epilepsy (Picciotto *et al.* 1995; Cordero-Erausquin *et al.* 2000; Jensen *et al.* 2005).

nAChR β4 subunit mRNA colocalizes in different species with α4 subunit mRNA in numerous brain regions (Winzer-Serhan & Leslie, 1997; Quik *et al.* 2000) implicated in complex behaviours, including nicotine dependence. Knock-out studies suggest that nAChR containing β2 or β4 subunits in mouse brain play different roles. For example, in nAChR β2(−/−) animals, nicotine fails to elicit striatal dopamine release, fails to increase (at concentrations similar to those found in the arterial blood of human smokers) discharge frequency of midbrain dopaminergic neurons, and fails to elicit self-administration, suggesting roles for

 DOI: 10.1113/jphysiol.2006.114645

nAChR-containing $\beta 2$ subunits in nicotine reinforcement (Picciotto *et al.* 1998). Although $\beta 2$ subunit substitution in $\beta 4(-/-)$ animals can prevent the perinatally lethal effects of autonomic failure seen in $\beta 2(-/-)/\beta 4(-/-)$ mice, $\beta 4(-/-)$ mice still exhibit autonomic dysfunction (Wang *et al.* 2003), have heightened resistance to nicotine-induced seizures (Kedmi *et al.* 2004), and have decreased nicotine withdrawal symptoms (Salas *et al.* 2004). Heterologous expression in *Xenopus* oocytes of rat nAChR $\alpha 2$, $\alpha 3$ or $\alpha 4$ subunits in pairwise combination with either $\beta 2$ or $\beta 4$ subunits produces nAChR having differing nicotinic agonist binding affinities attributable to the β subunit assembly partner (Parker *et al.* 1998). As part of a literature demonstrating functional heterologous expression of functional nAChR-containing $\beta 4$ subunits, rat nAChR $\beta 2$ or $\beta 4$ subunits influence kinetics of whole-cell current decay phase (Fenster *et al.* 1997) and sensitivity to competitive nicotinic antagonists and Zn^{2+} modulation (Harvey & Luetje, 1996). Moreover, heterologously expressed, rat $\alpha 2\beta 4$- or $\alpha 3\beta 4$-nAChR show an unusual functional potentiation in the presence of D-tubocurarine at lower concentrations (1–10 μM) than those needed to inhibit nicotinic responses (Cachelin & Rust, 1994).

To establish a foundation for studies of the possible roles of human $\alpha 4\beta 4$-nAChR in addition to $\alpha 4\beta 2$-nAChR in mediation of classic cholinergic excitatory neurotransmission, in modulation of neurotransmitter release, and/or in neuropsychiatric diseases, and to enhance understanding of roles played by β subunits in nAChR structure and function, patch-clamp recording of whole-cell currents was used to undertake a systematic comparison of functional properties of human $\alpha 4\beta 2$- and $\alpha 4\beta 4$-nAChR heterologously expressed in the SH-EP1 human epithelial cell line. Our results show clear distinctions between these nAChR in desensitization kinetics, affinities and efficacies of nicotinic ligands, and current–voltage relationships, demonstrating important influences of β subunits on $\alpha 4^*$-nAChR function.

Methods

Expression of human neuronal $\alpha 4\beta 2$- and $\alpha 4\beta 4$-nAChR in SH-EP1 human epithelial cells

Human $\alpha 4$ and $\beta 2$ or $\beta 4$ subunits (kindly provided by Dr Ortrud Steinlein or Jon Lindstrom) were subcloned into pcDNA3.1-zeocin and pcDNA3.1-hygromycin vectors, respectively, and transfected using established techniques (Puchacz *et al.* 1994; Peng *et al.* 1999, 2005) into native nAChR-null SH-EP1 cells (Lukas *et al.* 1993) following the approach taken to create the SH-EP1-h$\alpha 4\beta 2$ cell line (Eaton *et al.* 2003) in order to generate the SH-EP1-h$\alpha 4\beta 4$ cell-line (Eaton *et al.* 2000). Briefly, three million SH-EP1 cells in 0.5 ml of 20 mM Hepes, 87 mM NaCl, 5 mM KCl, 0.7 mM NaH_2PO_4, 6 mM dextrose, pH 7.05, in an electroporation cuvette, were mixed with 100 μg of vector DNA containing the $\beta 4$ subunit insert. Samples were subjected to electroporation (Bio-Rad Gene Pulsar model 1652076, Richmond, CA, USA) at 960 μF and 200 V. After electroporation, cells were suspended to 5 ml in complete medium (Bencherif & Lukas, 1993), and 1 ml aliquots were added to 12 ml aliquots of medium in each of five 100 mm dishes. Forty-eight hours later, positive selection was initiated in medium supplemented with 0.4 mg ml^{-1} hygromycin (Calbiochem, La Jolla, CA, USA). The polyclonal pool of surviving cells was harvested and subjected to a second round of transfection via electroporation with vector DNA containing the $\alpha 4$ subunit insert and selected for zeocin (0.5 mg ml^{-1}; Invitrogen, Carlsbad, CA, USA) resistance beginning 48 h later. Colonies of surviving cells were picked, subcloned by limiting dilution, and expanded before being screened for radioligand binding and functional evidence for $\alpha 4\beta 4$-nAChR expression, which led to selection of the clone designated as the SH-EP1-h$\alpha 4\beta 4$ cell line. Cells were maintained as low passage number (1–26 from our frozen stocks) cultures, to ensure stable expression of phenotype, maintained in medium augmented with 0.5 mg ml^{-1} zeocin and 0.4 mg ml^{-1} hygromycin, and passaged once weekly by splitting just-confluent cultures 1/10 to maintain cells in proliferative growth.

RNA preparation and reverse transcription polymerase chain reaction (RT-PCR)

Total RNA was isolated from the cells growing at approximately 80% confluence in a 100 mm culture dish using 2 ml of Trizol reagent (Bethesda Research Laboratories, Gaithersburg, MD, USA). Prior to RT-PCR, RNA preparations were treated with amplification-grade, RNase-free DNase (Bethesda Research Laboratories, Gaithersburg, MD, USA) in order to remove residual genomic DNA contamination. Typically, 1 μg of RNA was incubated with 1 unit of DNaseI in a 10 μl reaction at room temperature for 15 min, and then the DNase was inactivated by addition of 1 μl of 25 mM EDTA and incubated at 65°C for 10 min. RT was carried out using 0.8 μg of DNA-free total RNA, oligo $d(T)_{12-18}$ primer, and the Superscript II Preamplification system (Bethesda Research Laboratories, Gaithersburg, MD, USA) in a 20 μl reaction. At the end of the RT reaction, reverse transcriptase was deactivated by incubation at 75°C for 10 min, and RNAs were removed by adding 1 unit of RNaseH followed by incubation at 37°C for 30 min. A typical PCR was performed using 2 μl of cDNA preparation, 1 μl of 10 μM each of 5′- and 3′-gene-specific primers, 1 μl of 10 mM dNTP, and 2.5 units of RedTaq (Sigma, St. Louis, MO, USA) in a 50 μl reaction. The primers used in the amplification stage were designed and synthesized based on published gene

sequences (GenBank accession number: α4 NM000744, β2 NM009602, β4 NM000750; GAPDH BC026907). The primer sequences and their predicted product sizes are: α4 sense 5′-GAATGTCACCTCCATCCGCATC-3′, α4 antisense 5′-CCGGCA(A/G)TTGTC(C/T)TTGACCAC-3′ (product size 790 bp); β2 sense 5′-CGGCTCCCTTCCAAACACA-3′, β2 antisense 5′-GCAATGATGGCGTGGCTGCTGCA-3′ (product size 754 bp); β4 sense 5′-TCTGGTTGCCTGACATCGTG-3′, β4 antisense 5′-GGGTTCACAAAGTACATGGA-3′ (product size 847 bp); GAPDH sense 5′-CGTATTGGGCGCCTGGTCACCAG-3′, GAPDH antisense 5′-GTCCTTGCCCACAGCCTTGGCAGC-3′ (product size 624 bp). Amplification reactions were carried out in a RoboCycler (Stratagene, La Jolla, CA, USA) for 35 amplification cycles at 95°C for 1 min, 55°C for 90 s, and 72°C for 90 s, followed by an additional 4-min extension at 72°C. One-tenth of each RT-PCR product was then resolved on a 1% agarose gel, and sizes of products were determined based on migration relative to mass markers loaded adjacently.

Immunolabelling of nAChR α4 subunit in SH-EP1 cells

nAChR subunits on the surface of SH-EP1- hα4β2 and non-transfected SH-EP1 controls were immunolabelled with a rat monoclonal antibody against the nAChR α4 subunit (clone 299; Covance, Berkeley, CA, USA). Live, unfixed, non-permeabilized cells were exposed (4°C, 1 h) to primary antibody diluted in PBS containing 5% bovine serum albumin (BSA; Sigma Chemical, St Louis, MO, USA), followed by fluorescent, antirat secondary antibody (Jackson ImmunoResearch, West Grove, PA, USA) for 1 h. Cells were then fixed (2% formaldehyde in PBS, 4°C, 30 min), dehydrated (methanol, −30°C, 5 min), air-dried, and mounted in ProLong antifade medium (Molecular Probes/Invitrogen, Carlsbad, CA, USA).

Samples were examined with a Zeiss Axiovert microscope using a 100×, high-NA objective for fluorescence, and digital images were collected with a Photometrics cooled CCD camera. Images were processed with Photoshop (Adobe Systems, San Jose, CA, USA) using the same settings for different samples.

Patch-clamp recordings

Conventional patch-clamp whole-cell current recordings coupled with techniques for fast application and removal of drugs (U-tube) were applied in this study as previously described (Wu *et al.* 1996, 2002, 2004*a* and *b*; Zhao *et al.* 2003). Briefly, cells plated on polylysine-coated 35-mm culture dishes were placed on the stage of an inverted microscope (Olympus IX7, Lake Success, NY, USA) and continuously superfused with standard external solution (2 ml min^{-1}). Glass microelectrodes (1.5 × 100 mm, Narishige, East Meadow, NY, USA) were made in two steps using a vertical electrode puller (P-830, Narishige, East Meadow, NY, USA). Electrodes with a resistance of 3–5 MΩ between the pipette and external solutions were used to form tight seals (>1 GΩ) on the cell surface, until suction was applied in order to convert to conventional whole-cell recording. Thereafter, the recorded cell was lifted and then voltage clamped at a holding potential (V_H) of −60 mV (unless specifically mentioned), and ionic currents in response to application of nicotinic ligands were measured (Axopatch 200B amplifier, Axon Instruments, Union City, CA, USA). Whole-cell access resistance was less than 20 MΩ before series resistance compensation. Both pipette and whole-cell current capacitances were minimized, and series resistance was routinely compensated to 80%. Typically, data were acquired at 10 kHz, filtered at 2 kHz, displayed and digitized online (Digidata 1322 series A/D board, Axon Instruments), and stored to hard drive. Data acquisition and analyses of whole-cell currents were done using Clampex9.2 (Axon Instruments), and results were plotted using Origin 5.0 (OriginLab Corp., North Hampton, MA, USA) or Prism 3.0 (GraphPad Software, Inc., San Diego, CA, USA). Concentration–response curves were fitted to the Hill equation. nAChR acute desensitization was analysed for decay time constant (τ), peak current (I_p), and steady-state current (I_s) using fits to the expression

$$I = \left[(I_p - I_s)e^{-t/\tau}\right] + I_s$$

or to its bi-exponential variant as appropriate, using data from 90% to 10% of the period between the peak amplitude of the inward current and the termination of the typical 4 s period of agonist exposure. Replicate determinations of τ (a measure of the rate of acute desensitization) and I_s/I_p (a measure of the extent of acute desensitization) are presented as means ± standard errors (S.E.M.), and comparisons of τ and I_s/I_p values across different conditions were analysed for statistical significance using the Student's *t* test (paired or independent). All experiments were performed at room temperature (22 ± 1°C).

Solutions and drug application

The standard external solution contained (mM): 120 NaCl, 3 KCl, 2 $MgCl_2$, 2 $CaCl_2$, 25 D-glucose, 10 Hepes, pH adjusted to 7.4 with Tris-base. In some experiments using ACh as an agonist, 1 μM atropine sulphate was added to the standard solution to exclude any possible influences of muscarinic receptors, but the results were the same as those obtained in the absence of atropine (data not shown). Three types of pipette solutions were used for conventional whole-cell recording. Electrodes containing (mM): 140 KCl, 4 $MgCl_2$, 1 $CaCl_2$, 0.5 EGTA, 4 Na-ATP, 10 Hepes, pH adjusted to 7.2 with KOH (K^+ electrodes)

were used to examine current–voltage relationships. Electrodes containing (mM): 120 CsCl, 30 NaCl, 4 $MgCl_2$, 1 $CaCl_2$, 0.5 EGTA, 4 Na-ATP, 10 Hepes, pH adjusted to 7.2 with KOH (Cs^+ electrodes) were used in some cases to further compare inward rectification between $\alpha4\beta2$- and $\alpha4\beta4$-nAChR. This pipette solution was used for two reasons: (a) replacing K^+ with Cs^+ increased recording stability at more positive V_H values, and (b) increasing the Na^+ concentration (from 4 to 34 mM) showed more clear outward currents at positive V_H values. Electrodes containing (mM): 110 Tris phosphate dibasic, 28 Tris base, 11 EGTA, 2 $MgCl_2$, 0.1 $CaCl_2$, 4 Na-ATP, pH 7.3 ($Tris^+$ electrodes; Huguenard & Prince, 1992) were used for other experiments, since this pipette solution was reported to prevent receptor functional rundown (Zhao *et al.* 2003).

To initiate whole-cell current responses, under constant superfusion of the recording chamber, nicotinic drugs were rapidly delivered to the recorded cell using a computer-controlled 'U-tube' application system. Using this device, the rising time (10–90%) for junction potential effects induced by applied diluted external solution (50% distilled water) was 8.3 ms, and rising times for 1 mM ACh-induced whole-cell currents ($V_H = -60$ mV, lifted whole-cell recording) were 10.9 ± 1.1 ms ($n = 15$) and 39.2 ± 2.1 ms ($n = 8$) for $\alpha4\beta2$-nAChR and $\alpha4\beta4$-nAChR, respectively. In some experiments, a fast-step drug application system (SF-77B, Warner Ins. Co., Hamden, USA) was used. With minimal movement of it (100 μm), the rising time for junction potential effects was 3.0 ms, and the rising times for 1 mM ACh-induced whole-cell currents ($V_H = -60$ mV, lifted whole-cell recording) were 10.8 ± 1.2 ms ($n = 9$) and 33.9 ± 3.2 ms ($n = 9$) for $\alpha4\beta2$-nAChR and $\alpha4\beta4$-nAChR, respectively. Intervals between drug applications (3 min) were adjusted specifically to ensure stability of nAChR responsiveness (absence of functional rundown), and the selection of pipette solutions used in most of the studies described here was made with the same objective. Drugs used in the present study were (−)nicotine, ACh, epibatidine, cytisine, lobeline, dihydro-β-erythroidine (DHβE), mecamylamine (MEC), hexamethonium (HEXA), D-tubocurarine (dTC), and methyllycaconitine (MLA) (Sigma Chemical Co., St. Louis, MO, USA).

Results

Evidence for expression of nAChR subunits in transfected SH-EP1 cells

SH-EP1 cells exhibit a range of morphologies before (not shown) or after (Fig. 1*A*) transfection with nAChR subunits. Reverse transcription-polymerase chain reaction (RT-PCR) analyses showed expression of human nAChR $\alpha4$ and $\beta2$ subunit messages in SH-EP1-h$\alpha4\beta2$ cells, and expression of human $\alpha4$ and $\beta4$ subunit messages in SH-EP1-h$\alpha4\beta4$ cells (Fig. 1*B*). By contrast, there was no such expression in the absence of the reverse transcription step or in the untransfected cell host, despite successful amplification of GAPDH message in all of the cells (Fig. 1*B*). Immunocytochemical staining using a monoclonal anti-nAChR $\alpha4$ subunit antibody showed bright, punctate, specific labelling on the surfaces of transfected SH-EP1-h$\alpha4\beta2$ cells (Fig. 1C*b*; see phase contrast image at lower power in Fig. 1*Ca*) but no specific labelling on untransfected cells (Fig. 1*Cc*) or SH-EP1-h$\alpha4\beta2$ cells exposed only to secondary antibody (Fig. 1*Cd*). These results indicated appropriate expression of nAChR subunits from cDNAs as messages and as cell surface protein in stably transfected SH-EP1 cells.

Distinctive properties of functional $\alpha4\beta2$- and $\alpha4\beta4$-nAChR

Whole-cell current recording using $Tris^+$ electrodes revealed the expression of functional $\alpha4\beta2$- or $\alpha4\beta4$-nAChR in transfected SH-EP1-h$\alpha4\beta2$ or SH-EP1-h$\alpha4\beta4$ cells responding to nicotine (Fig. 2). One obvious difference in whole-cell response profiles depending on the nAChR β subunit assembly partner was the kinetics and extent of whole-cell current decay from peak to steady-state levels during a single exposure to nicotine. We operationally define this process as nAChR acute desensitization. The rate of acute desensitization was much slower for $\alpha4\beta4$-nAChR than for $\alpha4\beta2$-nAChR, and the extent of whole-cell current decline was smaller for $\alpha4\beta4$-nAChR than for $\alpha4\beta2$-nAChR (Fig. 2*A* and *B*). Another obvious difference was the higher amplitude of $\alpha4\beta4$-nAChR responses (peak and steady-state) to low (around EC_{50}; see below) or high (100 μM) concentrations of nicotine (Fig. 2*A* and *B*). Results obtained from studies of SH-EP1 cells each expressing either $\alpha4\beta2$- ($n = 31$) or $\alpha4\beta4$-nAChR ($n = 31$) confirm the higher amplitude responses mediated by $\alpha4\beta4$-nAChR after normalizing inward current to cell capacitance (16.3 ± 1.6 pA pF^{-1} current density for $\alpha4\beta2$-nAChR; 41.3 ± 5.7 pA pF^{-1} for $\alpha4\beta4$-nAChR; Fig. 2*Ca*). Across those cells, in the presence of EC_{50} concentrations of nicotine, the average ratio of steady-state/peak currents was $34 \pm 1\%$ for $\alpha4\beta2$-nAChR and $85 \pm 2\%$ for $\alpha4\beta4$-nAChR (Fig. 2*Cb*), and the average time required for an e-fold rise inward current was 59 ± 3 ms for $\alpha4\beta2$-nAChR and 107 ± 6 ms for $\alpha4\beta4$-nAChR, reflecting faster opening of $\alpha4\beta2$-nAChR channels (Fig. 2*Cc*). The average time constants for e-fold decline in nicotine-induced whole-cell current from peak values were 440 ± 50 ms for $\alpha4\beta2$-nAChR (nicotine 3 μM, $n = 20$) and 2480 ± 160 ms for $\alpha4\beta4$-nAChR (nicotine 1 μM, $n = 18$, Fig. 2*Cd*), reflecting the faster and more extensive acute desensitization of $\alpha4\beta2$- compared to

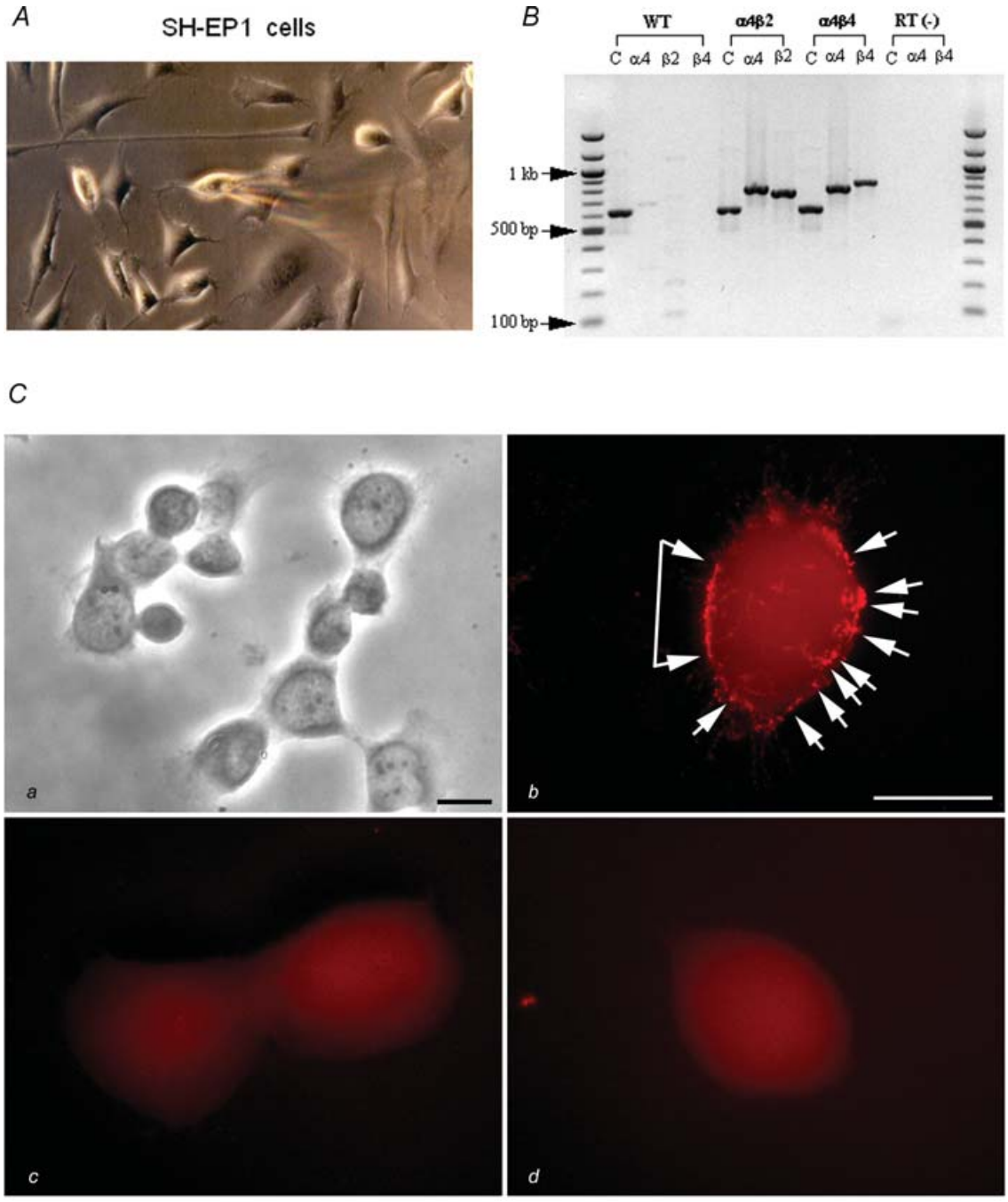

Figure 1. Morphology and transgene expression in SH-EP1 cells
A, phase-contrast photomicrograph of transfected SH-EP1 cells during patch-clamp recording. *B*, RT-PCR analysis of α4, β2 or β4 nAChR subunit transcripts or GAPDH internal controls (C) from wild-type (*WT*) SH-EP1 cells or from cells cotransfected with α4 plus either β2 ($\alpha4\beta2$) or β4 ($\alpha4\beta4$) subunits. Lanes labelled 'RT(−)' are for samples from SH-EP1-h$\alpha4\beta4$ cells processed after omission of the RT step. Sizes of RT-PCR products resolved on a 1% agarose gel are calibrated using a 100-bp DNA ladder (New England BioLabs Inc., Beverly, MA, USA). *C*, immunolabelling of nAChR α4 subunits on SH-EP1-h$\alpha4\beta2$ cells. *Ca*, low-magnification, phase-contrast view of SH-EP1-h$\alpha4\beta2$ cells. *Cb*, high-magnification, fluorescence view of a SH-EP1-h$\alpha4\beta2$ cell labelled with rat monoclonal antibody 299 against the nAChR α4 subunit. *Cc*, non-transfected SH-EP1 cells labelled with the same antibody as in *B*. *Cd*, a SH-EP1-h$\alpha4\beta2$ cell labelled with secondary antibody only. Note the bright, punctate, specific labelling (arrows in panel *Cb*) on the surface of SH-EP1-h$\alpha4\beta2$ cells and the absence of specific labelling on non-transfected cells and SH-EP1-h$\alpha4\beta2$ cells exposed only to secondary antibody. Bars in *Ca* and *Cb* represent 5 μm; bar in *Cb* applies to panels *Cb*–*Cd*.

$\alpha4\beta4$-nAChR. These effects were not artifacts of the rate of drug delivery, and the lower amplitude of the peak current response mediated by $\alpha4\beta2$-nAChR was not a consequence of the faster desensitization of those receptors. Whole-cell current densities induced in the presence of a lower concentration of nicotine (100 nM) that produced no clear desensitization of either receptor were 1.99 ± 0.36 pA pF^{-1} ($n = 7$) for $\alpha4\beta2$-nAChR and 4.72 ± 0.66 pA pF^{-1} ($n = 7$, $P < 0.01$) for $\alpha4\beta4$-nAChR, preserving the >2-fold higher response of $\alpha4\beta4$-nAChR compared to $\alpha4\beta2$-nAChR.

During recording using a K^+ electrode, repeated exposures of a SH-EP1 cell expressing $\alpha4\beta2$-nAChR to nicotine at its EC_{50} concentration (see below) for 4 s at 1 min intervals caused a gradual reduction in peak current amplitudes, which we operationally define as functional rundown (Fig. 3*A* and *C*). By contrast, the same protocol for repeated challenge with nicotine did not produce functional rundown of $\alpha4\beta4$-nAChR-mediated currents (Fig. 3*B* and *C*). These results indicate that nAChR $\beta2$ or $\beta4$ subunits play important roles in determining functional rundown of $\alpha4^*$-nAChR.

Nicotinic agonist actions at $\alpha4\beta2$- and $\alpha4\beta4$-nAChR

$\alpha4\beta2$- and $\alpha4\beta4$-nAChR-mediated whole-cell currents induced by different concentrations of nicotine were recorded using $Tris^+$ electrodes at a V_H of -60 mV (Fig. 4*A* and *B*). Absolute (Fig. 4*C*) or normalized (to the response to 100 μM nicotine; Fig. 4*D*) peak whole-cell current responses to nicotine when plotted as a function of nicotine concentration were sigmoidal and well-fitted by a single-site model of the logistic equation (with no improvement in fit using a two-site model). Fits to the data yielded EC_{50} values and Hill coefficients of 3.1 μM (2.0–4.7 μM; 95% confidence interval) and 0.78 ± 0.09 (S.E.M.), respectively, for $\alpha4\beta2$-nAChR ($n = 10$ cells), and 1.3 μM (0.72–2.20 μM) and 1.18 ± 0.27, respectively,

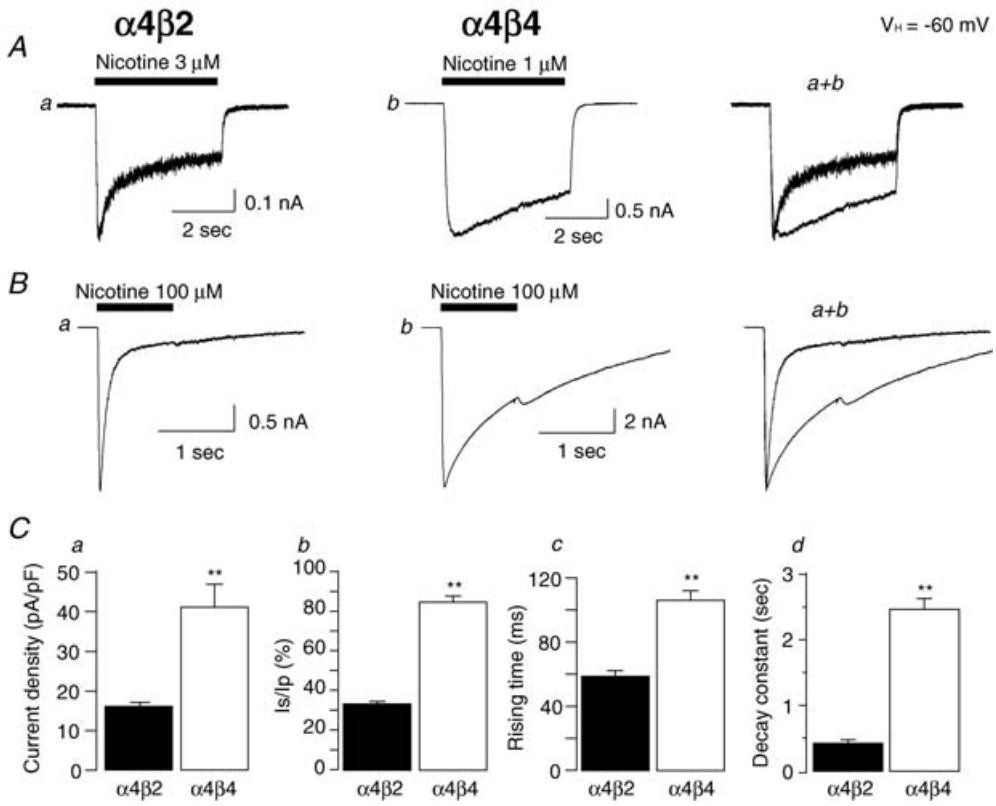

Figure 2. Electrophysiological properties of $\alpha4\beta2$- and $\alpha4\beta4$-nAChR
Low (3 or 1 μM, *A*) or high (100 μM, *B*) concentrations of nicotine were applied to induce whole-cell inward currents in transfected SH-EP1 cells stably expressing human $\alpha4\beta2$- (*Aa* and *Ba*) or $\alpha4\beta4$- (*Ab* and *Bb*) nAChR. Superimposed traces from each row are shown in the right column. *C*, bar graphs summarizing results of replicate studies (31 cells each) illustrating differences between $\alpha4\beta2$- (filled bars) and $\alpha4\beta4$- (open bars) nAChR responses in net current density (*a*), the ratio of steady-state to peak components (*b*), the rising time to peak whole-cell current (*c*) and whole-cell current decay constant (*d*). Data were averaged from 31 cells tested for Fig. 2 *Ca*-*c*, and 18 cells tested for $\alpha4\beta4$-nAChR and 20 cells tested for $\alpha4\beta2$-nAChR in Fig. 2*Cd*, and vertical bars represent S.E.M. $^{**}P < 0.01$ for difference between $\alpha4^*$-nAChR subtypes. All data presented in Fig. 2*C* were obtained from whole-cell currents induced by equipotent concentrations of 3 μM nicotine ($\alpha4\beta2$-nAChR) or 1 μM nicotine ($\alpha4\beta4$-nAChR).

for $\alpha4\beta4$-nAChR ($n = 7$ cells; Fig. 4*D*). Moreover, peak current amplitude was about 5-fold higher for $\alpha4\beta4$- than for $\alpha4\beta2$-nAChR (Fig. 4*C*). These findings demonstrated both higher efficacy (Fig. 4*C*) and affinity (Fig. 4*D*) for nicotine acting at human $\alpha4\beta4$-nAChR compared to $\alpha4\beta2$-nAChR (Table 1). Whole-cell peak current response profiles for other nicotinic agonists, including cytisine (Fig. 5*A*), lobeline (Fig. 5*B*) and epibatidine (EPBD) (Fig. 5*C*), were obtained and normalized to the maximal response to nicotine (at 100 μM; Fig. 5*A–C*, columns *a* and *b*). These profiles indicate partial (~20%) efficacy of cytisine and lobeline (compared to maximal effects of nicotine or ACh) at $\alpha4\beta2$-nAChR, but nearly full or full efficacy at $\alpha4\beta4$-nAChR, whereas epibatidine acts as a full agonist at both $\alpha4\beta2$- and $\alpha4\beta4$-nAChR. When responses to individual agonists were normalized to their own maximal effect at a given $\alpha4^*$-nAChR subtype (Fig. 5*A–C*, column *c*), it was evident that EC_{50} values for cytisine were about 6-fold lower and EC_{50} values for nicotine, ACh, lobeline or epibatidine were about 2.4- to 3.4-fold lower for actions at $\alpha4\beta4$-nAChR compared to actions at $\alpha4\beta2$-nAChR (Table 1). Rank-order agonist potency (EC_{50} values and 95% confidence intervals provided in parentheses) is epibatidine (0.100 μM; 0.03–0.36) ≫ cytisine (1.3 μM; 0.79–2.20) ≥ nicotine (3.1 μM; 2.0–4.7) = lobeline (3.1 μM; 2.5–3.9) ≥ ACh (4.1 μM; 3.2–5.0) for $\alpha4\beta2$-nAChR, and epibatidine (0.029 μM; 0.020–0.043) > cytisine (0.21 μM; 0.14–0.33) > nicotine (1.3 μM; 0.72–2.20) = lobeline (1.3 μM; 0.73–2.30) ≥ ACh (1.7 μM; 1.2–2.4) for $\alpha4\beta4$-nAChR. These results indicate that cytisine or lobeline act on $\alpha4\beta2$-nAChR as partial agonists, but act on $\alpha4\beta4$-nAChR as full agonists, providing a means for distinguishing between $\alpha4^*$-nAChR subtypes in addition to generally higher agonist potency at $\alpha4\beta4$-nAChR (Table 1).

Nicotinic antagonist actions at $\alpha4\beta2$- and $\alpha4\beta4$-nAChR

The effects of selected nicotinic antagonists on function of $\alpha4\beta2$- and $\alpha4\beta4$-nAChR elicited by EC_{50} concentrations of nicotine were assessed using $Tris^+$ electrode recording. DHβE coapplied with

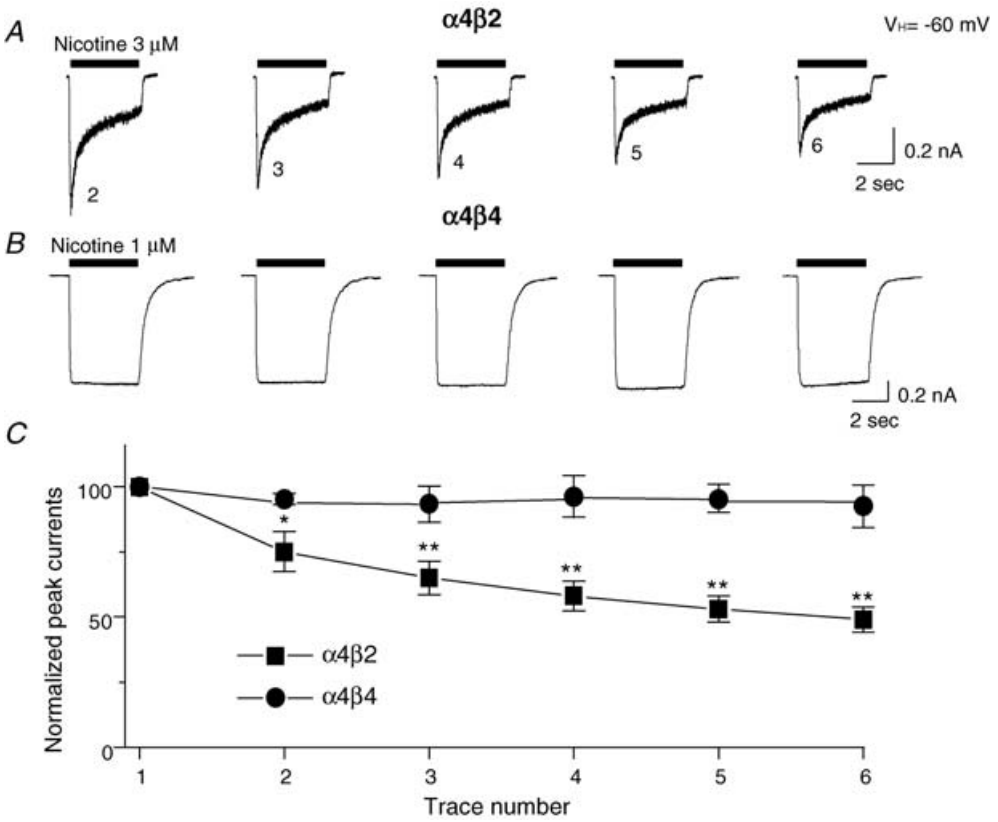

Figure 3. Functional rundown of $\alpha4\beta2$- and $\alpha4\beta4$-nAChR
Using K^+ electrodes at a V_H of −60 mV, 3 or 1 μM nicotine was repetitively applied for 4 s at 1-min intervals to SH-EP1 cells expressing either $\alpha4\beta2$- (*A*) or $\alpha4\beta4$- (*B*) nAChR, respectively. Peak current components from whole-cell current traces are plotted against trace number in (*C*) for $\alpha4\beta2$- (■) or $\alpha4\beta4$- (●) nAChR. Each symbol represents the average from six cells tested, and vertical bars represent S.E.M. $^*P < 0.05$; $^{**}P < 0.01$.

Table 1. Profiles for agonist interactions with $\alpha4\beta2$- and $\alpha4\beta4$-nAChR

	$\alpha4\beta2$			$\alpha4\beta4$		
	log EC_{50}	Hill coefficient	*n*	log EC_{50}	Hill coefficient	*n*
Nicotine	-5.51 ± 0.07	0.78 ± 0.09	10	-5.90 ± 0.10	1.18 ± 0.27	7
ACh	-5.39 ± 0.04	0.87 ± 0.07	7	-5.77 ± 0.06	1.91 ± 0.42	6
Epibatidine	-6.98 ± 0.26	0.59 ± 0.13	6	-7.54 ± 0.08	0.58 ± 0.05	6
Cytisine	-5.88 ± 0.10	0.62 ± 0.09	6	-6.67 ± 0.08	0.80 ± 0.08	7
Lobeline	-5.51 ± 0.04	0.85 ± 0.05	5	-5.89 ± 0.10	1.19 ± 0.28	6

Whole-cell current recording was done as described in Methods and in the legends to Figs 4 and 5 as a function of agonist concentration. Peak whole-cell currents elicited were plotted against log molar agonist concentration, and the results were fitted to the logistic equation to determine log EC_{50} values and Hill coefficients (±S.E.M.) as indicated for either $\alpha4\beta2$- or $\alpha4\beta4$-nAChR. Also shown are the numbers of cells from which data were analysed.

nicotine reduced both peak and steady-state current responses of both $\alpha4\beta2$- and $\alpha4\beta4$-nAChR in a concentration-dependent manner (Fig. 6*A* and *B*). Similar studies evaluated concentration-dependent effects of other antagonists on function of $\alpha4\beta2$- and $\alpha4\beta4$-nAChR (Fig. 6*C* and *D*, Table 2). As DHβE does, mecamylamine, D-tubocurarine and methyllycaconitine block nicotine-induced peak currents mediated through

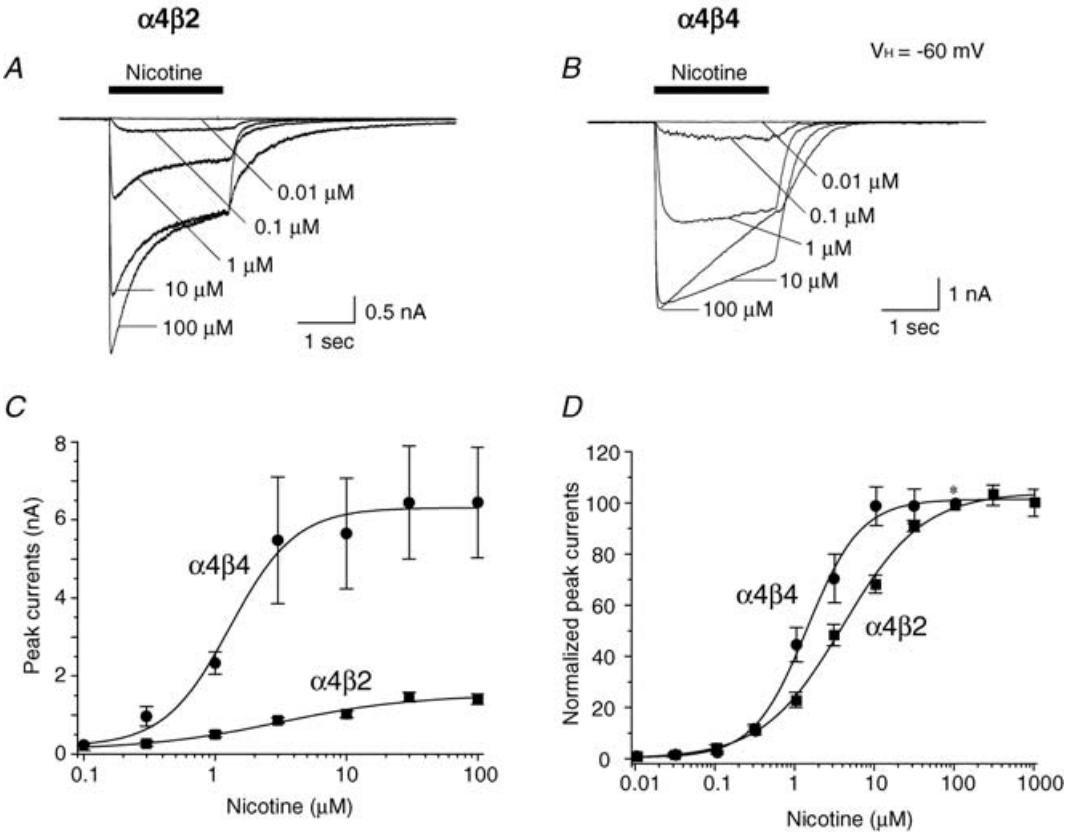

Figure 4. Nicotine concentration–response relationships for $\alpha4\beta2$- and $\alpha4\beta4$-nAChR
Five superimposed whole-cell current traces elicited in response to nicotine exposure (0.01–100 μM) are shown for cells expressing either $\alpha4\beta2$- (*A*) or $\alpha4\beta4$- (*B*) nAChR. *C*, nicotine alone (*) concentration–response curves plotted for absolute peak current values for $\alpha4\beta2$- (■) or $\alpha4\beta4$- (●) nAChR show differences in current amplitudes. *D*, nicotine concentration–response curves plotted for peak currents normalized to those evoked in response to 100 μM nicotine alone (*) show differences at $\alpha4\beta2$- (■) or $\alpha4\beta4$- (●) nAChR in agonist potency. In *C* and *D*, each symbol represents the average from 6–8 cells, and vertical bars represent S.E.M.

α4β2- or α4β4-nAChR, with largely similar inhibitory potencies (Table 2). Hexamethonium more potently blocks α4β2- than α4β4-nAChR function (Table 2). Rank-order inhibition potency (IC_{50} values and 95% confidence intervals provided in parentheses) is DHβE (0.89 μM; 0.72–1.10) ≫ mecamylamine (4.2 μM; 3.5–5.1) ≫ hexamethonium (30 μM; 21–42) ∼ methyllycaconitine (35 μM; 31–38) = D-tubocurarine (35 μM; 26–46) for α4β2-nAChR and DHβE (1.2 μM; 0.93–1.50) ≫ mecamylamine (4.9 μM; 3.2–7.4) > > methyllycaconitine (26 μM; 17–39) ≥ d-tubocurarine (50 μM; 37–68) > hexamethonium (91 μM; 74–110) for α4β4-nAChR.

Nicotine dose–response profiles were obtained alone or in the presence of 0.3 μM DHβE, 1 μM mecamylamine, or 0.5 μM hexamethonium (Fig. 7). In the presence of DHβE, nicotine concentration–response curves were predominantly shifted to the right without effects on the maximal response for both α4β2- and α4β4-nAChR, consistent with a competitive mechanism of functional block (Fig. 7*Aa* and *b*). Mecamylamine reduced the maximal current response without changing nicotine EC_{50} values, suggesting a non-competitive block (Fig. 7*Ba* and *b*). Interestingly, hexamethonium exhibited non-competitive block of α4β2-nAChR but displayed features of competitive block of α4β4-nAChR (Fig. 7*Ca* and *b*). These results suggest that classic competitive (DHβE) or non-competitive (mecamylamine) nicotinic antagonists have expected effects on both α4β2- and α4β4-nAChR, whereas the mechanism of hexamethonium block is probably different for α4β2- and α4β4-nAChR.

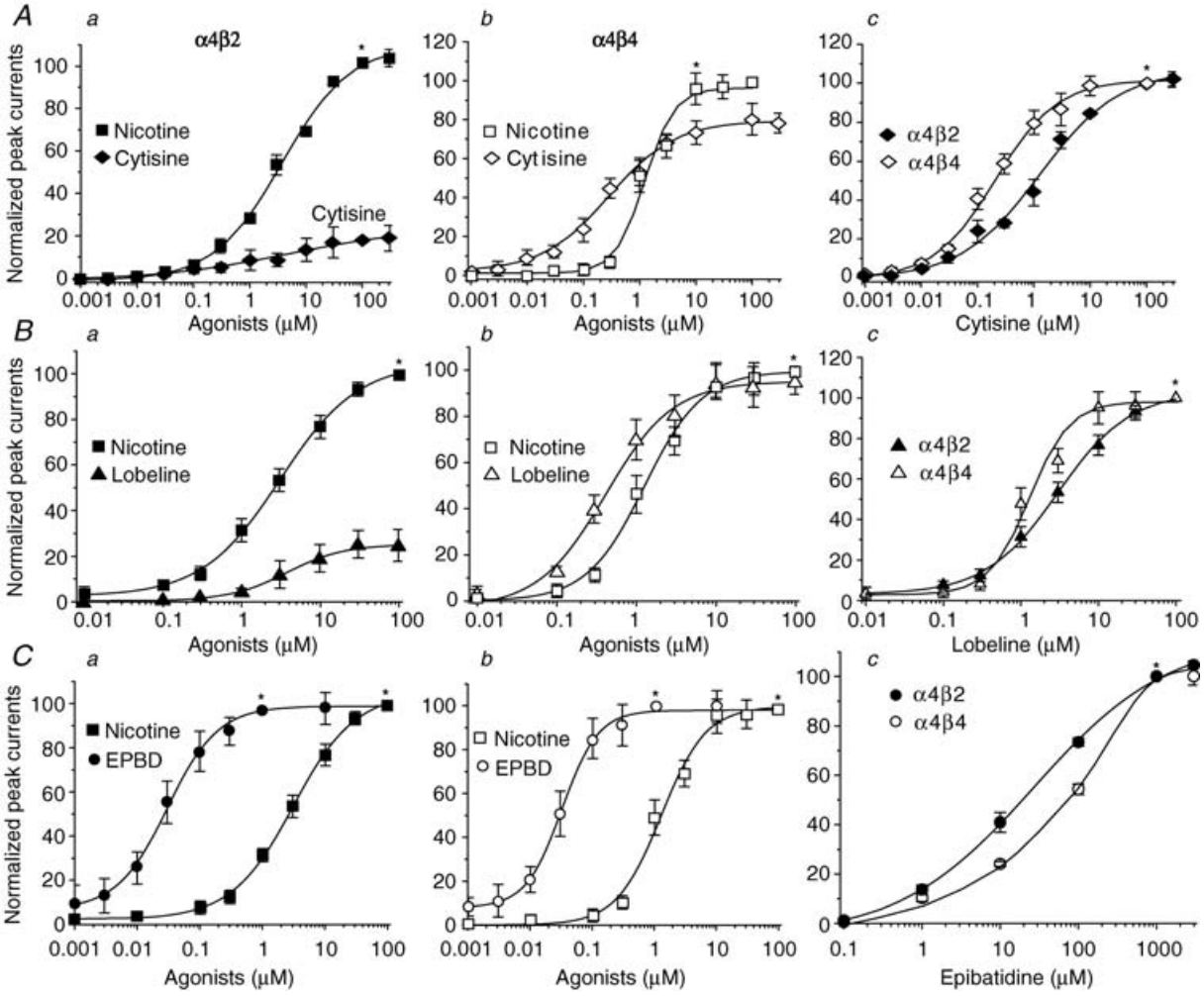

Figure 5. Concentration–response curves for cytisine, lobeline and epibatidine acting at α4β2- and α4β4-nAChR

Peak current responses of α4β2- (left column) or α4β4- (middle column) nAChR evoked by cytisine (*A*; ♦ or ◇), lobeline (*B;* ▲ or △), or epibatidine (EPBD) (*C;* ● or ○) are plotted after being normalized to the response evoked by 100 μM nicotine (■ or □; indicated by *) or (right column) responses of both α4*-nAChR subtypes to those drugs normalized to the maximal response to a given drug are plotted. Each symbol represents the average from 5 to 6 cells tested, and vertical bars represent standard errors.

Table 2. Comparison of antagonist properties of $\alpha4\beta2$- and $\alpha4\beta4$-nAChR

	$\alpha4\beta2$		$\alpha4\beta4$	
	log IC_{50}	Hill coefficient	log IC_{50}	Hill coefficient
DHβE	-6.05 ± 0.03	-1.45 ± 0.15	-5.92 ± 0.04	-1.16 ± 0.12
Mecamylamine	-5.38 ± 0.03	-1.29 ± 0.10	-5.31 ± 0.07	-0.69 ± 0.07
Hexamethonium	-4.53 ± 0.05	-0.67 ± 0.06	-4.04 ± 0.03	-0.65 ± 0.04
d-TC	-4.46 ± 0.04	-0.64 ± 0.05	-4.30 ± 0.05	-0.59 ± 0.04
Methyllycaconitine	-4.46 ± 0.02	-0.99 ± 0.04	-4.59 ± 0.07	-0.62 ± 0.07

Whole-cell current recording was done as described in Methods and in the legend to Fig. 6 as a function of antagonist concentration. Peak whole-cell currents elicited were plotted against log molar antagonist concentration, and the results were fitted to the logistic equation to determine log IC_{50} values and Hill coefficients (±S.E.M.) as indicated for either $\alpha4\beta2$- or $\alpha4\beta4$-nAChR. Data are averages for values determined from 5–7 cells.

Current–voltage relationships for $\alpha4\beta2$- and $\alpha4\beta4$-nAChR

Whole-cell current traces recorded using K^+ electrodes and obtained for 100 μM nicotine-induced activation of $\alpha4\beta2$-nAChR after stepwise changes in V_H prior to agonist application show full inward rectification at positive V_H (Fig. 8*Aa*), but when using the same protocol for $\alpha4\beta4$-nAChR responses, inward rectification at positive V_H was substantial but

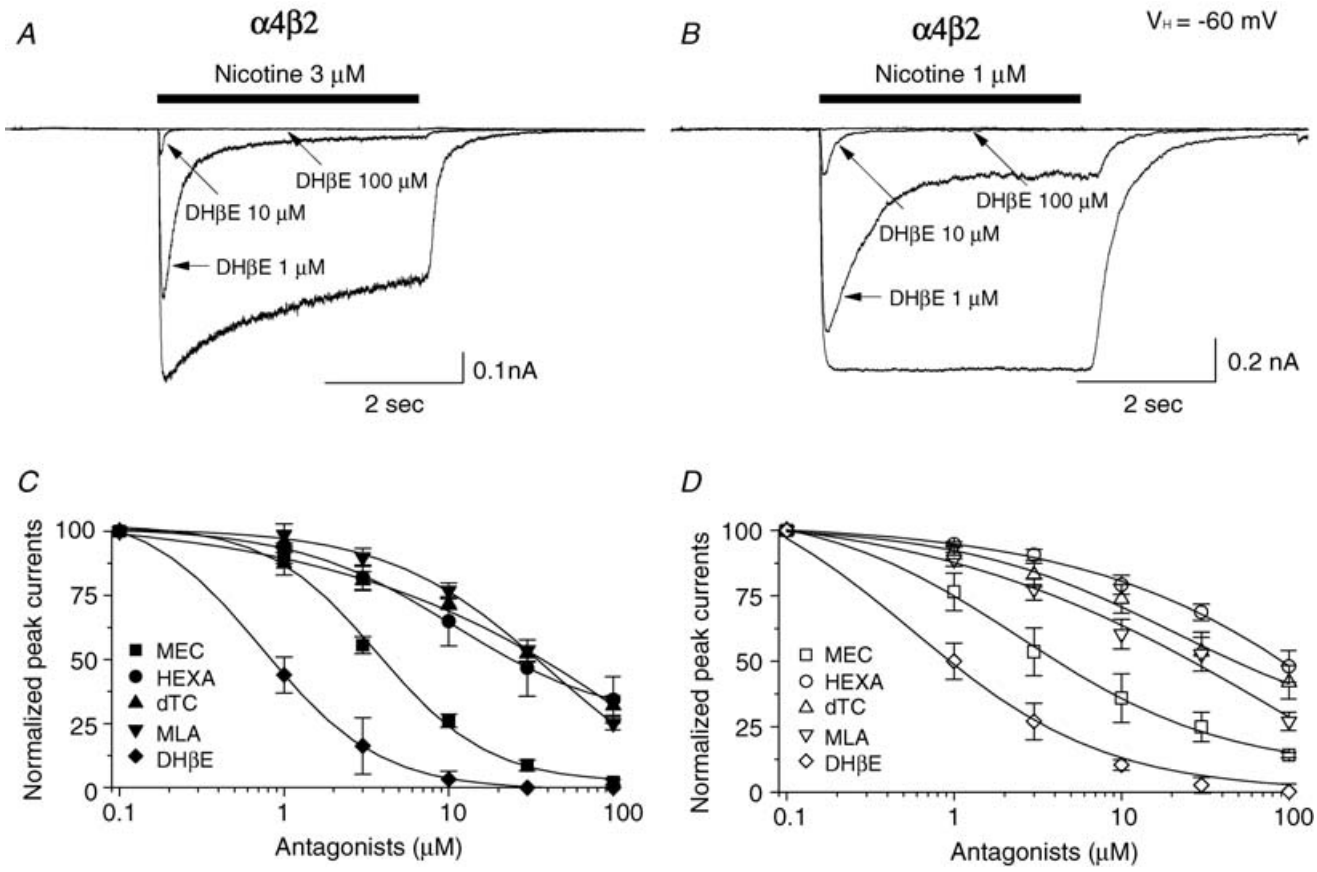

Figure 6. Antagonism of $\alpha4\beta2$- and $\alpha4\beta4$-nAChR function
3 μM (*A*) or 1 μM (*B*) nicotine (~EC_{50} concentration)-induced whole-cell currents obtained from exposure to SH-EP1-h$\alpha4\beta2$ (left) or -h$\alpha4\beta4$ (right) cells alone or in the presence of different concentrations of DHβE are superimposed. *C* and *D*, effects of coexposure to DHβE (♦, ◇), mecamylamine (MEC; ■, □), hexamethonium (HEXA; ●, ○), D-tubocurarine (d-TC; ▲, △) or methyllycaconitine (MLA; ▼, ▽) on nicotine-evoked whole-cell peak current responses of $\alpha4\beta2$- (3 μM nicotine, *C*) or $\alpha4\beta4$-nAChR (1 μM nicotine, *D*) are plotted as concentration–response curves. Each symbol represents the average from 5–6 cells, and vertical bars represent S.E.M.

incomplete (Fig. 8*Ab*). Results compiled from studies using six cells confirm that $\alpha4\beta4$-nAChR-mediated whole-cell currents exhibit less inward rectification than $\alpha4\beta2$-nAChR-mediated currents, suggesting roles for β subunits in the phenomenon (Fig. 8A*c*). In additional studies using pipette solutions containing 30 mM NaCl to enhance outward currents, responses to 1 mM ACh at V_H values between −80 and +100 mV were recorded for $\alpha4\beta2$- (Fig. 8*Ba*) and $\alpha4\beta4$-nAChR (Fig. 8*Bb*). Figure 8*Bc* summarizes the current–voltage relationship curves (from

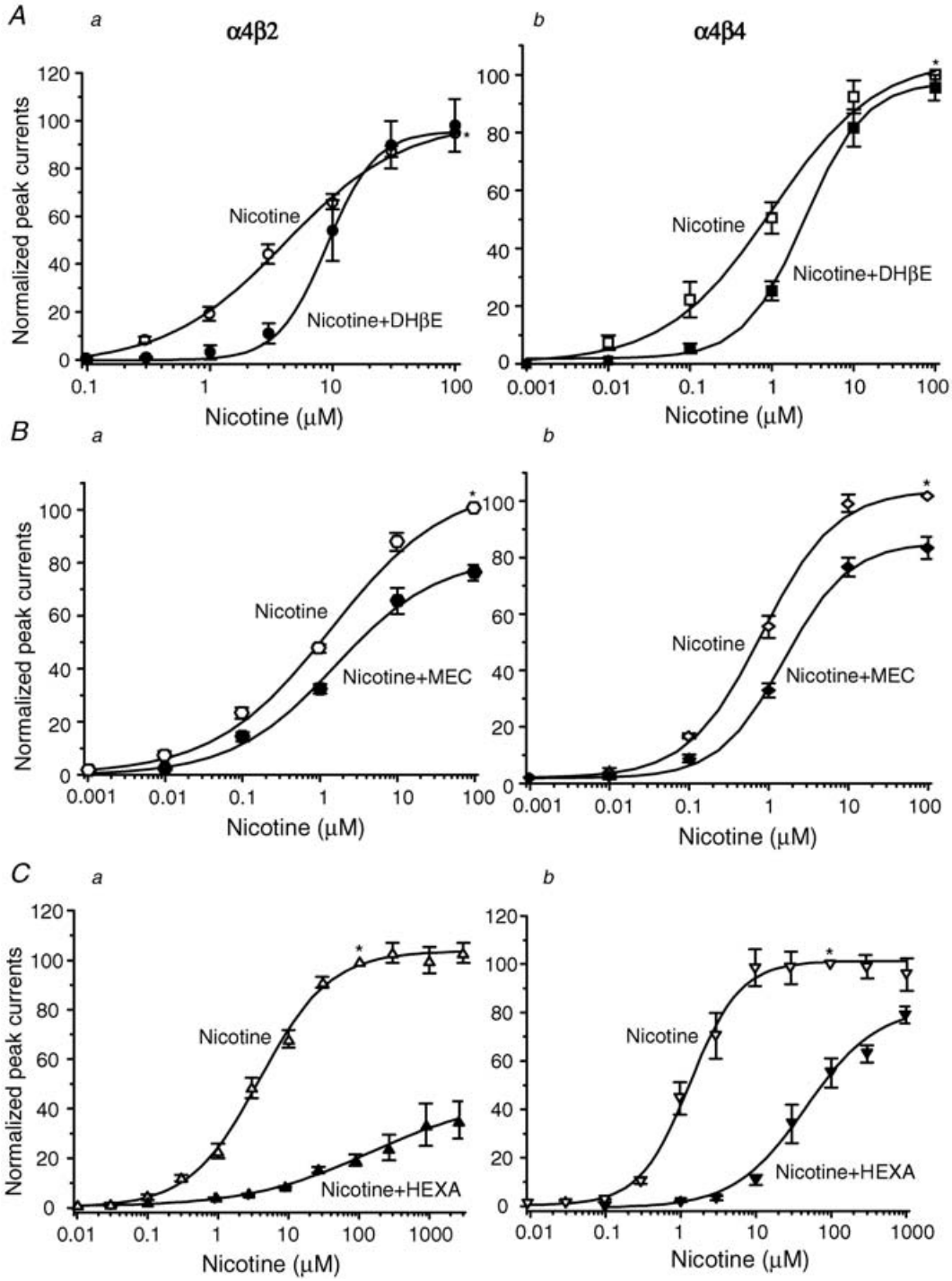

Figure 7. Comparison of antagonist action at $\alpha4\beta2$- and $\alpha4\beta4$-nAChR
Nicotine concentration–response curves alone or in the presence of 0.3 μM DHβE (*Aa*, $\alpha4\beta2$-nAChR; *Ab*, $\alpha4\beta4$-nAChR), 1 μM MEC (*Ba*, $\alpha4\beta2$-nAChR; *Bb*, $\alpha4\beta4$-nAChR) or 0.5 μM HEXA (*Ca*, $\alpha4\beta2$-nAChR; *Cb*, $\alpha4\beta4$-nAChR) are superimposed. All nicotinic responses were normalized to the current induced by 100 μM nicotine alone (*). Each symbol represents the average from 5–8 cells, and vertical bars represent S.E.M.

−80 to +100 mV) for $\alpha4\beta2$- and $\alpha4\beta4$-nAChR from six cells tested, and confirms weaker inward rectification for $\alpha4\beta4$-nAChR- than for $\alpha4\beta2$-nAChR-mediated whole-cell currents.

Discussion

The present study reveals differences between heterologously expressed, human $\alpha4\beta2$- and $\alpha4\beta4$-nAChR in agonist potencies and efficacies, in sensitivity to selected antagonists, in kinetics and amplitudes of whole-cell current responses, and in sensitivity to functional rundown and inward rectification. That is, when compared to $\alpha4\beta2$-nAChR, $\alpha4\beta4$-nAChR mediate responses that have higher whole-cell current density, exhibit a slower decay rate, are characterized by a smaller extent of acute desensitization, are subject to less functional rundown, and exhibit reduced inward rectification. Based on effects on peak whole-cell currents, nicotine, acetylcholine, cytisine, lobeline and epibatidine have higher functional potency at $\alpha4\beta4$-nAChR than at $\alpha4\beta2$-nAChR, but nicotinic antagonists have comparable functional inhibitory potency at both $\alpha4^*$-nAChR subtypes except for hexamethonium, which is a weaker antagonist of $\alpha4\beta4$-nAChR function. Hexamethonium has features more like a competitive antagonist at $\alpha4\beta4$-nAChR, but like a non-competitive blocker of $\alpha4\beta2$-nAChR function. Competitive or non-competitive mechanisms of block across $\alpha4^*$-nAChR subtypes are conserved for DHβE or mecamylamine, respectively. These results indicate that nAChR $\beta2$ or $\beta4$ subunits influence a number of properties, but not all features, of $\alpha4^*$-nAChR function.

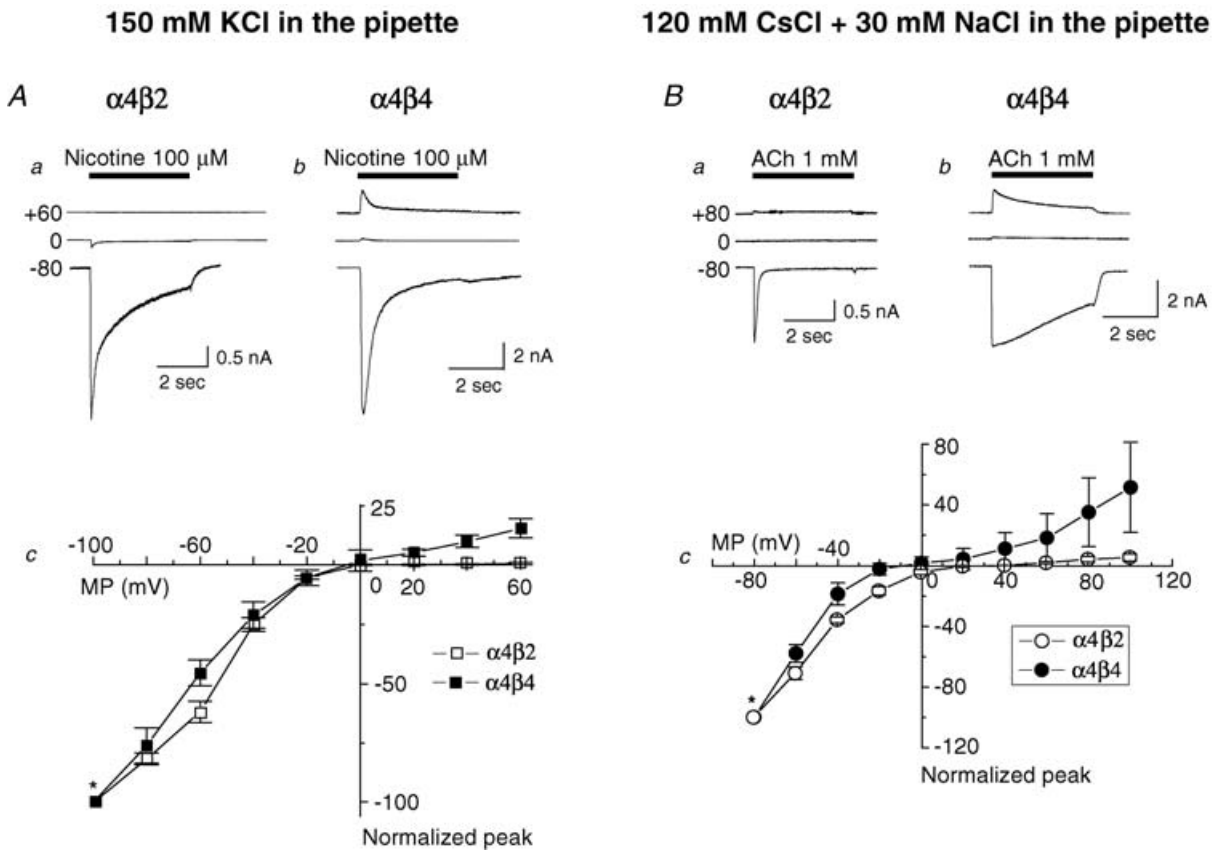

Figure 8. Current-voltage (*I–V*) relationships for $\alpha4\beta2$- and $\alpha4\beta4$-nAChR
A, whole-cell peak currents evoked by 100 μM nicotine (indicated by black horizontal bar) at different V_H values (−80, 0, +60 mV) are shown above current–voltage response curves normalized to the response to nicotine at −100 mV (*) for $\alpha4\beta2$- (*Aa*; □ in *Ac*) or $\alpha4\beta4$- (*Ab*; ■ in *Ac*) nAChR. Each symbol represents the average from six cells, and vertical bars (in *c*) represent S.E.M. *B*, sample traces for *I–V* curve analyses for $\alpha4\beta2$- (*a*) and $\alpha4\beta4$- (*b*) nAChR whole-cell current responses assessed using a higher (30 mM) concentration of Na^+ in the pipette solution evoked by 1 mM ACh (indicated by black horizontal bar) at different V_H values (−80, 0, +80 mV) are shown above current–voltage response curves normalized to the response to nicotine at −80 mV (*) for $\alpha4\beta2$- (*Ba*; ○ in (*Bc*) or $\alpha4\beta4$- (*Bb*; ● in *Bc*) nAChR.

β subunits influence sensitivity of α4*-nAChR to functional inactivation

Given that nAChR appear to undergo more than one phase of functional inactivation, we propose the use of at least two terms to describe these processes and refined approaches to tease them apart. 'Acute desensitization' is defined in the present study as it was by Ochoa *et al.* (1990): the loss in nAChR response during a single stimulus or exposure to agonist, reflecting decay of inward currents typically recorded from a cholinoceptive cell from a peak to a lower, steady-state level. Levels of acute desensitization can be quantified in terms of time or rate constants of the decay in response and by the ratio between steady-state and peak inward current responses. Provided that the duration of agonist exposure is limited, and that the time between agonist challenges is adequately long, full recovery should occur from acute desensitization within seconds to minutes. 'Functional rundown' is defined as the reduction in peak responses to agonist due to repetitive agonist exposures. Ochoa *et al.* (1990) provided an illustration (see their Fig. 3*B*), but not a specific definition, of functional rundown. By our definition, functional rundown can be quantified in terms of peak current amplitude either as a function of cumulative time of repetitive agonist exposures or of numbers of agonist exposures.

The current study addresses the roles of β subunits in α4*-nAChR acute desensitization and functional rundown. They show dramatically lower acute desensitization and functional rundown of α4β4-nAChR compared to α4β2-nAChR. The high conservation of amino acids across human β2 and β4 subunits in putative transmembrane domains, including the M2 domain thought to line the channel itself, suggests that alternative sites may be involved in differences in functional inactivation. One candidate is the second major cytoplasmic loop, changes in which influence nAChR acute desensitization (Kuo *et al.* 2005). The finding that there is slower desensitization of α4β4-nAChR than of α4β2-nAChR may have physiological and pathophysiological significance. For example, given their comparable sensitivity to nicotine, α4β4-nAChR would be more resistant to functional inactivation by nicotine than α4β2-nAChR (see Gentry *et al.* 2003), meaning they could play an important role in maintaining cholinergic network activity after chronic exposure to smoking-relevant nicotinic concentrations (100–500 nM), under conditions where other nAChR are either deeply desensitized (Pidoplichko *et al.* 1997) or not activated (Zhao *et al.* 2003). Consistent with such a perspective, β4-subunit knockout mice have altered nicotine withdrawal symptoms (Salas *et al.* 2004). Diversity in nAChR dependent on whether they contain β2 or β4 subunits (perhaps in combination with additional subunits from the family) thus could allow for different physiological outcomes relevant to nicotine reinforcement, dependence and withdrawal.

β subunits influence α4*-nAChR pharmacology

Many studies have indicated that mammalian brain α4β2-nAChR are the nAChR subtype with the highest binding affinity for nicotine (Benowitz *et al.* 1989; Hsu *et al.* 1995; Fenster *et al.* 1997; Lukas *et al.* 1999; Jensen *et al.* 2005; Lukas, 2006). In studies using nAChR heterologously expressed in the oocyte system, the binding affinity of ACh for rat α4β2-nAChR was 2-fold higher than for rat α4β4-nAChR (Parker *et al.* 1998). However, patch-clamp whole-cell recording using the same expression system showed a 2-fold higher functional agonist potency for ACh acting at α4β4-nAChR compared to α4β2-nAChR (Francis *et al.* 2000). Our results show that nicotine, epibatidine and ACh have ∼2.4–3.4-fold higher functional potency when acting at α4β4-nAChR than at α4β2-nAChR. Moreover, α4β4-nAChR have higher affinity than α4β2-nAChR for cytisine and lobeline, both of which are fully efficacious at α4β4-nAChR but are only partial agonists at α4β2-nAChR. Interestingly, radioligand binding studies indicate that human α4β2-nAChR have higher agonist-binding affinities than human α4β4-nAChR (Eaton *et al.* 2000), but this simply suggests that functional and binding assays may assess ligand interactions with different states (resting, desensitized) of the receptor. Thus, α4β2-nAChR remain as the highest affinity binding sites for nicotinic agonists when assessed using radioligand binding, but α4β4-nAChR have higher agonist affinities when surveyed using whole-cell (or ion flux; Eaton *et al.* 2000) assays.

Antagonist sensitivities of the two α4*-nAChR subtypes studied are similar for the agents tested except for hexamethonium, which engages in non-competitive block of α4β2-nAChR, but has a competitive and weaker inhibitor profile when acting at α4β4-nAChR. A caveat is that these experiments assessed the effects on whole-cell peak currents, which may or may not be the most important indicator of physiological or pharmacological status of nAChR *in vivo*. Nevertheless, from a potential therapeutic perspective, these studies suggest that nicotinic agonists selectively targeting α4β4-nAChR could be designed that would be much less efficacious and potent when acting at α4β2-nAChR, and perhaps diseases affecting nicotinic signalling and elements of nicotine dependence could be treated with better outcome by targeting α4β4-nAChR.

β subunits influence α4*-nAChR inward rectification

Inward rectification is an important functional feature of several ligand- and voltage-gated ion channels,

including $\alpha 4^*$-nAChR (Haghighi & Cooper, 1998), but the mechanisms involved remain unclear. It has been suggested that polyamine interactions with a subsite in the channel-lining domain of nAChR blocks the channel pore in a voltage-dependent manner, leading to receptor inward rectification (Haghighi & Cooper, 1998, 2000). Apparent inverse relationships between inward rectification and Ca^{2+} permeability have been suggested in other studies (Lewis, 1979; Adams *et al.* 1980; Hume *et al.* 1991; Verdoorn *et al.* 1991; Dingledine *et al.* 1999). Other models consider relationships between roles for intracellular K^+ in destabilization of polyamines with nAChR during depolarization and/or in outward ion flow (Washburn *et al.* 1997; Haghighi & Cooper, 1998). We have found that heterologously expressed, human $\alpha 4\beta 4$-nAChR show less inward rectification than $\alpha 4\beta 2$-nAChR, even when the intracellular Na^+ concentration is high. There is a previous report of lower Ca^{2+} permeability in $\beta 4$-containing than in $\beta 2$-containing nAChR (Haghighi & Cooper, 1998). However, further studies comparing $\alpha 4\beta 2$- and $\alpha 4\beta 4$-nAChR have promise with respect to elucidation of mechanisms engaged in inward rectification.

Potential physiological relevance of $\beta 4$-containing nAChR in the brain

nAChR $\beta 4$ subunits play clear roles as assembly partners with $\alpha 3$ subunits in $\alpha 3\beta 4^*$-nAChR that mediate *trans*-ganglionic signalling (Duvoisin *et al.* 1989; Rust *et al.* 1994; Xu *et al.* 1999). $\beta 4$ subunits also are expressed in the central nervous system as both mRNA and protein (Dineley-Miller & Patrick, 1992; Tarroni *et al.* 1992; Poth *et al.* 1997; Quick *et al.* 1999; Quik *et al.* 2000; Klink *et al.* 2001; Gahring *et al.* 2004). In several brain regions, including the basal ganglia, cerebellum, hippocampus and cortex, the $\beta 4$ subunit is a candidate assembly partner for the $\alpha 4$ subunit because $\alpha 3$ subunits are either absent or expressed at low levels (Dineley-Miller & Patrick, 1992). $\beta 4$ subunits are prominently expressed in thalamic somatosensory relay nuclei and in somatosensory cortex (Gahring *et al.* 2004), suggesting involvement in sensory processing. $\beta 4$-null mice have altered responses in anxiety-related tests (Salas *et al.* 2003) and upon nicotine withdrawal (Salas *et al.* 2004), and have higher resistance to nicotine-induced seizures (Kedmi *et al.* 2004). Dopamine neurons freshly dissociated from the rat ventral tegmental area express functional nAChR with properties suggestive of the presence of $\beta 4$ subunits that are expressed as mRNA in the same region (Wu *et al.* 2005). These putative $\beta 4^*$-nAChR mediate whole-cell current responses to ACh that are of higher amplitude (400–1000 pA) and desensitize more slowly than $\alpha 4\beta 2$-nAChR-mediated responses. These $\beta 4^*$-nAChR are sensitive to the nicotinic agonist cytisine, but insensitive to the $\alpha 4\beta 2$-nAChR-selective agonist RJR-2403 (Papke *et al.* 2000). In addition, these $\beta 4^*$-nAChR are highly sensitive to the nicotinic receptor antagonist mecamylamine, but show low sensitivity to the $\alpha 4\beta 2$-nAChR-selective antagonist DHβE. While the possibility is that these nAChR have a subunit composition more complicated than $\alpha 4$ plus $\beta 4$, the similarities between their properties and those of $\alpha 4\beta 4$-nAChR defined in the current study are striking, and involvement of $\beta 4$ subunits seems clear. Functional $\beta 4^*$-nAChR in midbrain dopamine neurons may contribute to nicotine-induced modulation of midbrain dopamine neuronal function.

In summary, human $\alpha 4\beta 2$- and $\alpha 4\beta 4$-nAChR heterologously expressed in human SH-EP1 cells exhibit distinctive physiological and pharmacological properties. Heterologous expression of these entities and identification of ways to distinguish them provide insights into roles of these two $\alpha 4^*$-nAChR subtypes in health and disease and as therapeutic targets.

References

Adams DJ, Smith SJ & Thompson SH (1980). Ionic currents in molluscan soma. *Annu Rev Neurosci* **3**, 141–167.

Bencherif M & Lukas RJ (1993). Cytochalasin modulation of nicotinic cholinergic receptor expression and muscarinic receptor function in human TE671/RD cells: a possible functional role of the cytoskeleton. *J Neurochem* **61**, 852–864.

Benowitz NL, Porchet H & Jacob P III (1989). Nicotine dependence and tolerance in man: pharmacokinetic and pharmacodynamic investigations. *Prog Brain Res* **79**, 279–287.

Cachelin AB & Rust G (1994). Unusual pharmacology of (+)-tubocurarine with rat neuronal nicotinic acetylcholine receptors containing beta 4 subunits. *Mol Pharmacol* **6**, 1168–1174.

Cordero-Erausquin M, Marubio LM, Klink R & Changeux J-P (2000). Nicotinic receptor function: perspectives from knockout mice. *Trends Pharm Sci* **21**, 211–217.

Dineley-Miller K & Patrick J (1992). Gene transcripts for the nicotinic acetylcholine receptor subunit, beta4, are distributed in multiple areas of the rat central nervous system. *Brain Res Mol Brain Res* **16**, 339–344.

Dingledine R, Borges K, Bowie D & Traynelis SF (1999). The glutamate receptor ion channels. *Pharmacol Rev* **1**, 7–61.

Duvoisin RM, Deneris ES, Patrick J & Heinemann S (1989). The functional diversity of the neuronal nicotinic acetylcholine receptors is increased by a novel subunit: beta 4. *Neuron* **3**, 487–496.

Eaton JB, Kuo Y-P, Fuh LP-T, Krishnan C, Steinlein O, Lindstrom JM & Lukas RJ (2000). Properties of stably and heterologously-expressed human $\alpha 4\beta 4$-nicotinic acetylcholine receptors (nAChR). *Soc Neurosci Abstract* **26**, 371.

Eaton JB, Peng J-H, Schroeder KM, George AA, Fryer JD, Krishnan C, Buhlman L, Kuo Y-P, Steinlein O & Lukas RJ (2003). Characterization of human $\alpha 4\beta 2$-nicotinic acetylcholine receptors stably and heterologously expressed in native nicotinic receptor-null SH-EP1 human epithelial cells. *Mol Pharmacol* **64**, 1283–1294.

Fenster CP, Rains MF, Noerager B, Quick MW & Lester RAJ (1997). Influence of subunit compositions on desensitization of neuronal acetylcholine receptors at low concentrations of nicotine. *J Neurosci* **17**, 5747–5759.

Flores CM, Rogers SW, Pabreza LA, Wolfe BB & Kellar KJ (1992). A subtype of nicotinic cholinergic receptor in rat brain is composed of $\alpha 4$ and $\beta 2$ subunits and is up-regulated by chronic nicotine treatment. *Mol Pharmacol* **41**, 31–37.

Francis MM, Vazquez RW, Papke RL & Oswald RE (2000). Subtype-selective inhibition of neuronal nicotinic acetylcholine receptors by cocaine is determined by the alpha4 and beta4 subunits. *Mol Pharmacol* **58**, 109–119.

Gahring LC, Persiyanov K & Rogers SW (2004). Neuronal and astrocyte expression of nicotinic receptor subunit beta4 in the adult mouse brain. *J Comp Neurol* **468**, 322–333.

Gentry CL, Wilkins LH jr & Lukas RJ (2003). Effects of prolonged nicotinic ligand exposure on function of heterologously expressed, human $\alpha 4\beta 2$- and $\alpha 4\beta 4$-nicotinic acetylcholine receptors. *J Pharmacol Exper Ther* **304**, 206–216.

Gopalakrishnan M, Monteggia LM, Anderson DJ, Molinari EJ, Lattoni-Kaplan M, Donnelly-Roberts D, Arneric SP & Sullivan JP (1996). Stable expression, pharmacologic properties and regulation of the human neuronal nicotinic acetylcholine $\alpha 4\beta 2$ receptor. *J Pharmacol Exper Ther* **276**, 289–297.

Haghighi AP & Cooper E (1998). Neuronal nicotinic acetylcholine receptors are blocked by intracellular spermine in a voltage-dependent manner. *J Neurosci* **18**, 4050–4062.

Haghighi AP & Cooper E (2000). A molecular link between inward rectification and calcium permeability of neuronal nicotinic acetylcholine alpha3beta4 and alpha4beta2 receptors. *J Neurosci* **20**, 529–541.

Harvey SC & Luetje CW (1996). Determinants of competitive antagonist sensitivity on neuronal nicotinic receptor beta subunits. *J Neurosci* **16**, 3798–3806.

Hsu Y-N, Amin J, Weiss DS & Wecker L (1995). Sustained nicotine exposure differentially affects $\alpha 3\beta 2$ and $\alpha 4\beta 2$ neuronal nicotine receptors expressed in *Xenopus* oocytes. *J Neurochem* **66**, 667–675.

Huguenard JG & Prince DA (1992). A novel T-type current underlies prolonged Ca^{2+}-dependent burst firing in GABAergic neurons of rat thalamic reticular nucleus. *J Neurosci* **12**, 3804–3817.

Hume RI, Dingledine R & Heinemann SF (1991). Identification of a site in glutamate receptor subunits that controls calcium permeability. *Science* **253**, 1028–1031.

Jensen AA, Frolund B, Liljefors T & Krogsgaard-Larsen P (2005). Neuronal nicotinic acetylcholine receptors: Structural revelations, target identifications, and therapeutic inspirations. *J Med Chem* **48**, 4705–4745.

Kedmi M, Beaudet AL & Orr-Urtreger A (2004). Mice lacking neuronal nicotinic acetylcholine receptor beta4-subunit and mice lacking both alpha5- and beta4-subunits are highly resistant to nicotine-induced seizures. *Physiol Genomics* **17**, 221–229.

Klink R, de Kerchove d'Exaerde A, Zoli M & Changeux JP (2001). Molecular and physiological diversity of nicotinic acetylcholine receptors in the midbrain dopaminergic nuclei. *J Neurosci* **21**, 1452–1463.

Kuo Y-P, Xu L, Eaton JB, Zhao L, Wu J & Lukas RJ (2005). Roles for nicotinic acetylcholine receptor subunit large cytoplasmic loop sequences in receptor expression and function. *J Pharmacol Exper Ther* **314**, 455–466.

Lewis CA (1979). Ion-concentration dependence of the reversal potential and the single channel conductance of ion channels at the frog neuromuscular junction. *J Physiol* **286**, 417–445.

Lindstrom J (1996). Neuronal nicotinic acetylcholine receptors. In *Ion Channels*, Vol. 4, ed. Narahashi T, pp. 377–450. Plenum Press, New York.

Lukas RJ (2006). Pharmacological effects of nicotine and nicotinic receptor subtype pharmacological profiles. In *Medication Treatments for Nicotine Dependence*, ed. George TP. CRC Press, Boca Raton. pp. 3–23, in press.

Lukas RJ, Changeux J-P, Novère N, Le Albuquerque EX, Balfour DJK, Berg DK, Bertrand D, Chiappinelli VA, Clarke PBS, Collins AC, Dani JA, Grady SR, Kellar KJ, Lindstrom JM, Marks MJ, Quik M, Taylor PW & Wonnacott S (1999). International Union of Pharmacology. XX. Current status of the nomenclature for nicotinic acetylcholine receptors and their subunits. *Pharmacol Rev* **51**, 397–401.

Lukas RJ, Norman SA & Lucero L (1993). Characterization of nicotinic acetylcholine receptors expressed by cells of the SH-SY5Y human neuroblastoma clonal line. *Mol Cell Neurosci* **4**, 1–12.

Ochoa ELM, Li L & McNamee MG (1990). Desensitization of central cholinergic mechanisms and neuroadaptation to nicotine. *Mol Neurobiol* **4**, 251–287.

Papke RL, Webster JC, Lippiello PM, Bencherif M & Francis MM (2000). The activation and inhibition of human nicotinic acetylcholine receptor by RJR-2403 indicate a selectivity for the alpha4beta2 receptor subtype. *J Neurochem* **75**, 204–216.

Parker MJ, Beck A & Luetje CW (1998). Neuronal nicotinic receptor beta2 and beta4 subunits confer large differences in agonist binding affinity. *Mol Pharmacol* **54**, 1132–1139.

Peng J-H, Fryer JD, Hurst RS, Schroeder KM, George AA, Morrissy S, Groppi V, Leonard SS & Lukas RJ (2005). High-affinity epibatidine binding of functional, human $\alpha 7$-nicotinic acetylcholine receptors stably and heterologously expressed *de novo* in human SH-EP1 cells. *J Pharmacol Exper Ther* **313**, 24–35.

Peng J-H, Lucero L, Fryer J, Herl J, Leonard SS & Lukas RJ (1999). Inducible, heterologous expression of human $\alpha 7$-nicotinic acetylcholine receptors in a native nicotinic receptor-null human clonal line. *Brain Res* **825**, 172–179.

Picciotto MR, Zoli M, Lena C, Bessis A, Lallemand Y, Novere N, Le Vincent P, Pich EM, Brulet P & Changeux J-P (1995). Abnormal avoidance learning in mice lacking functional high-affinity nicotine receptor in the brain. *Nature* **374**, 65–67.

Picciotto MR, Zoli M, Rimondini R, Lena C, Marubio LM, Pich EM, Fuxe K & Changeux JP (1998). Acetylcholine receptors containing the beta2 subunit are involved in the reinforcing properties of nicotine. *Nature* **391**, 173–177.

Pidoplichko VI, DeBiasi M, Williams JT & Dani JA (1997). Nicotine activates and desensitizes midbrain dopamine neurons. *Nature* **390**, 401–404.

Poth K, Nutter TJ, Cuevas J, Parker MJ, Adams DJ & Luetje CW (1997). Heterogeneity of nicotinic receptor class and subunit mRNA expression among individual parasympathetic neurons from rat intracardiac ganglia. *J Neurosci* **17**, 586–596.

Puchacz E, Buisson B, Bertrand D & Lukas RJ (1994). Functional expression of nicotinic acetylcholine receptors containing rat α7 subunits in human neuroblastoma cells. *FEBS Lett* **354**, 155–159.

Quick MW, Ceballos RM, Kasten M, McIntosh JM & Lester RA (1999). Alpha3beta4 subunit-containing nicotinic receptors dominate function in rat medial habenula neurons. *Neuropharmacology* **38**, 769–783.

Quik M, Polonskaya Y, Gillespie A, Jakowec M, Lloyd GK & Langston JW (2000). Localization of nicotinic receptor subunit mRNAs in monkey brain by *in situ* hybridization. *J Comp Neurol* **425**, 58–69.

Rust G, Burgunder JM, Lauterburg TE & Cachelin AB (1994). Expression of neuronal nicotinic acetylcholine receptor subunit genes in the rat autonomic nervous system. *Eur J Neurosci* **6**, 478–485.

Salas R, Pieri F & De Biasi M (2004). Decreased signs of nicotine withdrawal in mice null for the beta4 nicotinic acetylcholine receptor subunit. *J Neurosci* **24**, 10035–10039.

Salas R, Pieri F, Fung B, Dani JA & De Biasi M (2003). Altered anxiety-related responses in mutant mice lacking the beta4 subunit of the nicotinic receptor. *J Neurosci* **16**, 6255–6263.

Tarroni P, Rubboli F, Chini B, Zwart R, Oortgiesen M, Sher E & Clementi F (1992). Neuronal-type nicotinic receptors in human neuroblastoma and small-cell lung carcinoma cell lines. *FEBS Lett* **312**, 66–70.

Verdoorn TA, Burnashev N, Monyer H, Seeburg PH & Sakmann B (1991). Structural determinants of ion flow through recombinant glutamate receptor channels. *Science* **252**, 1715–1718.

Wang N, Orr-Urtreger A, Chapman J, Rabinowitz R & Korczyn AD (2003). Deficiency of nicotinic acetylcholine receptor beta 4 subunit causes autonomic cardiac and intestinal dysfunction. *Mol Pharmacol* **63**, 574–580.

Washburn MS, Numberger M, Zhang S & Dingledine R (1997). Differential dependence on GluR2 expression of three characteristic features of AMPA receptors. *J Neurosci* **17**, 9393–9406.

Whiting PJ & Lindstrom J (1987). Purification and characterization of a nicotinic acetylcholine receptor from rat brain. *Proc Natl Acad Sci U S A* **84**, 595–599.

Winzer-Serhan UH & Leslie FM (1997). Co-distribution of nicotinic acetylcholine receptor subunit α3 and β4 mRNAs during rat brain development. *J Comp Neurol* **386**, 540–554.

Wu J, George AA, Schroeder KM, Xu L, Marxer-Miller S, Lucero L & Lukas RJ (2004*b*). Electrophysiological, pharmacological and molecular evidence for α7-nicotinic acetylcholine receptors in rat midbrain dopamine neurons. *J Pharmacol Exp Ther* **311**, 80–91.

Wu J, Harata N & Akaike N (1996). Potentiation by sevoflurane of the $GABA_A$-induced Cl- current in acutely dissociated CA1 pyramidal neurons from rat hippocampus. *Br J Pharmacol* **119**, 1013–1021.

Wu J, Hu J, Marxer-Miller S, Lucero L & Lukas RJ (2005). Diversity of functional nicotinic receptor subtypes in VTA dopamine neurons. *Soc Neurosci Abstract* **723**, 15.

Wu J, Kuo YP, George AA, Xu L, Hu J & Lukas RJ (2004*a*). β-amyloid directly inhibits human $\alpha4\beta2$-nicotinic acetylcholine receptors heterologously expressed in human SH-EP1 cells. *J Biol Chem* **279**, 37842–37851.

Wu J, Zhao L, Eaton JB & Lukas RJ (2002). Intracellular K^+ effluxes through activated nicotinic acetylcholine receptor/channels contributing to acute desensitization in human neuronal $\alpha4\beta2$-nAChR heterologously expressed in the SH-EP1 human epithelial cells. *Soc Neurosci Abstract* **617**, 8.

Xu W, Orr-Urtreger A, Nigro F, Gelber S, Sutcliffe CB, Armstrong D, Patrick JW, Role LW, Beaudet AL & De Biasi M (1999). Multiorgan autonomic dysfunction in mice lacking the beta2 and the beta4 subunits of neuronal nicotinic acetylcholine receptors. *J Neurosci* **19**, 9298–9305.

Zhao L, Kuo YP, George AA, Peng JH, Purandare MS, Schroeder KM, Lukas RJ & Wu J (2003). Functional properties of homomeric, human α7-nicotinic acetylcholine receptors heterologously expressed in the SH-EP1 human epithelial cell line. *J Pharmacol Exp Ther* **305**, 1132–1141.

Acknowledgements

Work toward this project, part of which was conducted in the Charlotte and Harold Simensky Neurochemistry of Alzheimer's Disease Laboratory, was supported by endowment and/or capitalization funds from the Men's and Women's Boards of the Barrow Neurological Foundation, the Robert and Gloria Wallace Foundation, and Epi-Hab Phoenix, Inc., and by grants from the National Institutes of Health (DA015389), the Arizona Disease Control (Biomedical) Research Commission (9615 and 9930), the Council for Tobacco Research (4366), the Marjorie Newsome and Sandra Solheim Aiken funds, and an Arizona Alzheimer's Disease Center pilot grant (P30 AG19610). The contents of this report are solely the responsibility of the authors and do not necessarily represent the views of the aforementioned awarding agencies.